Open Access

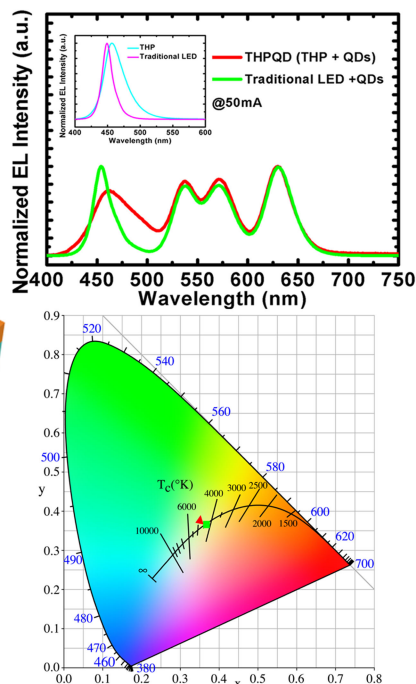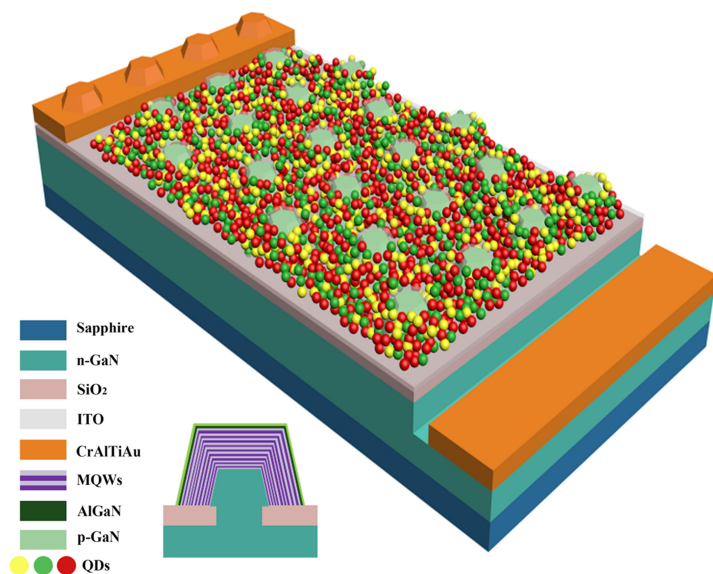# Phosphor-Free Three-Dimensional Hybrid White LED With High Color-Rendering Index

Jie Zhao
Tongbo Wei
Ji Zhang
Yonghui Zhang
Xuecheng Wei
Jianchang Yan
Junxi Wang
Jinmin Li

Phosphor-Free Three-Dimensional Hybrid White LED With High Color-Rendering Index

Jie Zhao,[1,2] Tongbo Wei [ID],[1,2] Ji Zhang,[3] Yonghui Zhang [ID],[3] Xuecheng Wei,[1,2] Jianchang Yan,[1,2] Junxi Wang,[1,2] and Jinmin Li[1,2]

[1]Semiconductor Lighting Technology Research and Development Center, Institute of Semiconductors, Chinese Academy of Sciences, Beijing 100083, China
[2]Center of Materials Science and Optoelectronics Engineering, University of the Chinese Academy of Sciences, Beijing 100049, China
[3]School of Electronics and Information Engineering, Hebei University of Technology, Tianjin 300401, China

Abstract: In this study, we demonstrate the phosphor-free hybrid white LED devices with the combination of the truncated-hexagonal-pyramid (THP) structures and quantum dots (QDs) (THPQD). In the THP structures, it is noted that the broad spectrum can be obtained from different microfacets. Moreover, the THP structures make the far-field viewing angle decrease by ∼45.4° and improve the light extraction efficiency compared with the traditional LED. The simulations also show that the light extraction efficiency of the THP LED is as approximately seven times as high as that of the traditional LED. Furthermore, by controlling the selective area growth (SAG) and adding QDs, the white emission can be realized from the THPQD LED with high color-rendering index (CRI). The CRI of the THPQD LED is from 71.2 up to 87.2 with the change of driving different current and its correlated color temperature covers the scope from 4845 to 5877 K.

Index Terms: Three-dimensional structures, quantum dots, phosphor-free, hybrid white LED, truncated-hexagonal-pyramid structures, light extraction efficiency, high color rendering index.

1. Introduction

In recent years, GaN-based white LEDs have received much attention and been widely used in solid-state lighting [1]–[3]. The LEDs have many advantages including small size, energy conservation, long lifetime, low power consumption, high efficiency and so on, which also can be used as the next generation light sources to replace the standard incandescent lamps [4]–[6]. To date, there are two methods to acquire white LEDs. One is the combination of red-green-blue (RGB) chips to emit white light, and the other is phosphor-converted (PC) LEDs by adding phosphors on top of blue or UV LED chips to enable white LEDs. The RGB-LEDs have the complicated feedback control system. For the PC-LEDs, because the wavelength conversion process occurs in the phosphors, their power and efficacy are usually reduced [7]. What's more, the PC-LEDs have a low color rendering index

owing to red emission deficiency in the visible spectrum. In addition, the PC-LEDs have other issues still to be required consideration such as the self-absorption of the phosphors, the low efficiency of the energy transfer from the blue or UV LEDs to the down-conversion phosphors, the degradation of phosphors, poor color-rendering index and so on [8]. In short, the white LEDs have received a great deal of attention and there are a few ways to obtain white LEDs without using phosphors.

Currently, in order to achieve phosphor-free white LEDs, dual-wavelength [9], [10] and three-dimensional (3D) [11], [12] GaN structures have been studied by using metal organic chemical vapor deposition (MOCVD). Especially, selective area growth (SAG) is a promising technique in creating semipolar and/or nonpolar GaN facets to fabricate white LEDs [13]. In principle, InGaN/GaN quantum well (QW) with suitable In contents and well widths can be used for covering the whole visible range. By SAG technology, 3D multifaceted GaN structures can be obtained, and highly-efficient long wavelength and white emission are realized. In addition, the white LEDs obtained by SAG technology to grow 3D structures have the several advantages: (1) The nonpolar and/or semipolar facets are exposed by SAG technology to grow 3D structures, and growing 3D structures also can incorporate different indium compared with traditional planar facet, which obtains broadband emission or multi-color emission [14]. (2) For higher In composition in the traditional (0001) c-plane QWs, there is a strong piezoelectric field, which causes the strong quantum confined Stark effect (QCSE), even leading to lower emission efficiency [15]. On the contrary, the QCSE can be reduced by using semipolar and/or nonpolar facets [16]–[18]. (3) The graphical interface can change the direction of optical beam in 3D structures, so that the more emitting light of total reflection has the opportunity to emit to the outside of the device [19], [20]. To date, by SAG technology, a series of 3D multifaceted GaN structures can be obtained, and highly-efficient long wavelength and nearly white emission are realized. Recently, Young-Ho Ko *et al.* realized the hexagonal annular structures [21] by SAG technology and Binglei Fu *et al.* tried the micro-pyramid structures [22] to obtain multi-color emission. Seung-Hyuk Lim *et al.* grew the pyramid structures with a truncated hexagonal pyramid surrounded by a hexagonal ring, which emitted nearly white emission with the color rendering index (CRI) value of R_a up to 75 [20]. In addition, there are hexagonal-annular-microrings structures with on Si-implanted GaN templates [23], concave-annular-microrings structures [24], dodecagonal ring structures [25] and so on. Although these 3D structures have different thicknesses and indium compositions in active region leading to broadband emission or multi-color emission, there are still severe CRI problems for them. In order to realize white light or nearly white light and achieve high CRI LEDs, it is necessary to get the proper polychromatic spectral distribution from the LEDs. The key issue is how to success in efficient green, yellow or red emissions.

To overcome the aforementioned problems, we demonstrate a phosphor-free hybrid white LED device with the combination of the truncated-hexagonal-pyramids (THP) structures and the quantum dots (QDs) (THPQD). This method not only can avoid the drawbacks of using phosphors, but also can tune the composition of In in the QW making the sidewall and the upper surface of the THP structures emit different lights. Furthermore, the high CRI hybrid LED can be achieved, with the value of from 71.2 up to 87.2 under driving different currents.

2. Experimental Details

In this experiment, phosphor-free hybrid white LEDs were grown on a c-plane (0001) sapphire substrate by MOCVD. After the deposition of a low-temperature nucleation layer, it was to grow the Si-doped n-GaN layer. To obtain the THP structures, a 200 nm thick SiO_2 mask layer was deposited on the c-plane n-GaN template. The holes were defined by the photolithographic mask. Then the n-GaN of the THP structures were grown at 1045 °C and 200 Torr followed by the active region. The active region consisted of nine periods of InGaN/GaN multiple quantum wells (MQWs) grown at 740 °C while the barriers were grown at a higher temperature of 810 °C under 250 Torr. Then AlGaN electron blocking layer and p-type doped GaN layer at 950 °C were epitaxially grown on MQWs. To fabricate THP LEDs, an indium-tin oxide (ITO) layer was deposited as a transparent current-spreading layer on the p-GaN layer. Then, the ITO was wet etched, p-GaN, MQWs and SiO_2 layers were etched away by inductively coupled plasma (ICP) until the n-GaN layer was exposed
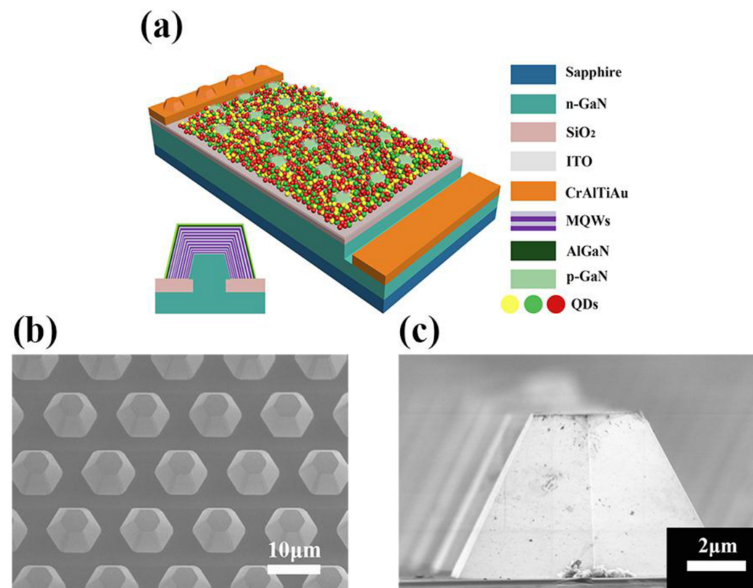
Fig. 1. (a) The schematic of the THPQD LED. (b) The top-view and (c) the cross-sectional SEM image of the THP arrays after the epitaxial process.

for n-type Ohmic contact formation. For the p-type and n-type electrodes, Cr/Al/Ti/Au layers were locally deposited on the surface of the ITO layer and the n-GaN layer, respectively. The fabricated THP chip size was 1.2 mm × 1.2 mm. The 530 nm (CdSe/ZnS core-shell), 570 nm (CdSe/ZnS core-shell) and 630 nm (CdSe/CdS/ZnS core-shell-shell) QDs (The diameters of the QDs are about 10 nm) were soluble in toluene to fabricate a certain ratio of QDs what we want. After mixing QDs with silicone resin, dispensing, curing at a higher temperature of 130 °C and blocking processes, a certain ratio of QDs were filled between the THP structures as shown in Fig. 1(a). The optical and electrical properties of the THP and THPQD LEDs were also discussed.

3. Results and Discussion

Fig. 1(b) shows the scanning electron microscopy (SEM) image of THP LED structures. It can be seen that the THP arrays are composed of six equivalent semipolar side facets and a c-plane (0001) because of the hexagonal wurtzite crystal symmetry of GaN. The morphology of the THP structures is almost identical, showing good homogeneity of growth process, while the GaN nucleation on the SiO_2 mask can be ignored. The angle between the inclined side facet and the bottom surface is approximately 62 degrees as shown in Fig. 1(c), meaning that the inclined side facet is the semipolar {10–11} side facet. The center-to-center distance between the THP structures is approximately 13 μm. The diameter of the THP structures is approximately 5 μm for the top surface and approximately 10 μm for the bottom surface, and the height is approximately 5.2 μm.

As shown in Fig. 2(a), the electroluminescence spectrum (EL) of the THP LED driven under different currents reveals the broadband and two-color emission of the THP LED, with a range of 425–550 nm. The light emitted has clearly changed from green to blue when the current is increased from 10 mA to 250 mA. At a relatively low current of 10 mA, the broad spectrum peak is produced from THP LED which is centered at about 480 nm (green peak). The blue peak appears at approximately 455 nm when the injection currents are higher than 50 mA. As the injection current further increases, the position of the green peak is blue-shifted due to Coulomb screening of the QCSE induced by the piezoelectric polarization and band filling effect [26]. However, the position
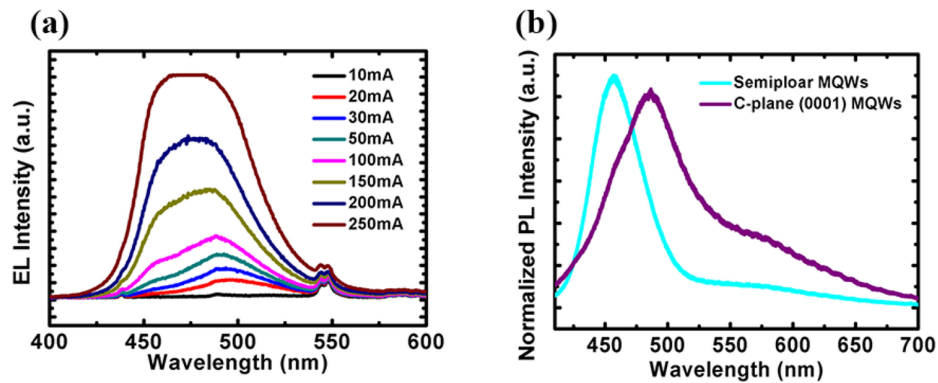
Fig. 2. (a) Typical EL spectrum of the THP LED driven under different currents. (b) The microscopic-PL spectrum of the THP microfacet structures.

of the blue peak is almost independent of the injection current. As the current increases, the peak intensity of the blue and green emissions both increases, but the peak intensity of the blue emission increases faster than the green emissions. This observation indicates that the two emission peaks may come from different areas within each THP structure.

To distinguish the origin of the blue and green emissions within THP structure, microscopic-photoluminescence (microscopic-PL) is measured under room temperature. The microfacets of the each THP structure are examined by microscopic-PL spectroscopy with a beam spot size of about 2 μm and the tested results are shown in Fig. 2(b). Here, two peak wavelengths come from InGaN/GaN MQWs grown on different microfacets. The peak wavelength from the MQWs on the {10–11} facet is approximately 455 nm, while the emission from MQWs on the c-plane (0001) shows longer wavelength of 480 nm. The c-plane (0001) is believed to have thicker InGaN well-thickness and higher In composition than semipolar {10–11} microfacets [27], because the diffusivity of indium atoms on the {10–11} side facets is larger than the c-plane (0001). Moreover, the {10–11} side-facets are made up of nitrogen terminated sites and the c-plane (0001) consists of gallium terminated sites, therefore the surface energy on the c-plane (0001) is lower than that of the {10–11} side-facets. In addition, the diffusivity of gallium atoms at the {10–11} side-facets is also larger than the c-plane (0001), similar to indium atoms as mentioned previously [28]. As a result, compared with the {10–11} side-facets, more indium atoms migrate into the c-plane (0001), and the total thickness of the active region on the c-plane (0001) is larger. In a word, the result of the microscopic-PL is good agreement with the result of EL, which reveals large polarization-induced electric fields in the MQWs grown on the c-plane (0001) GaN compared with those grown on semipolar facets.

To further explore the function of the THP structures, the light output angular distribution of the THP LED and traditional LED are measured at a driving current of 350 mA as shown in Fig. 3 and the intensity has been normalized. The viewing angles (where light emission intensity is 50% of the maximum) for the THP LED and traditional LED are ~95.3° and ~140.7°, respectively. The larger viewing angle observed for traditional LED implies that the light confined in the LED chip is extracted from edge of the chip or of the sapphire substrate after multiple scattering or reflection events [29]. For the THP LED, the light is effectively redirected to the top escape-cone of the LED through inclined sidewalls and SiO$_2$. Meanwhile, the light confined in the THP LED chip is extracted from the edge of the inclined sidewalls, THP structures serve as the diffraction layer and effectively redirect most of the light to the upper portion of the chip, resulting in the smaller viewing angle. The light extraction enhancement is considered as a consequence the combined effects of light wave guiding, surface texturing and geometrical shaping. To better understand the improvement of PHC on light extraction, we also use three-dimensional finite-difference time-domain (3D-TDFD) simulation to study the intrinsic nature of high light extraction efficiency of the THP LED.
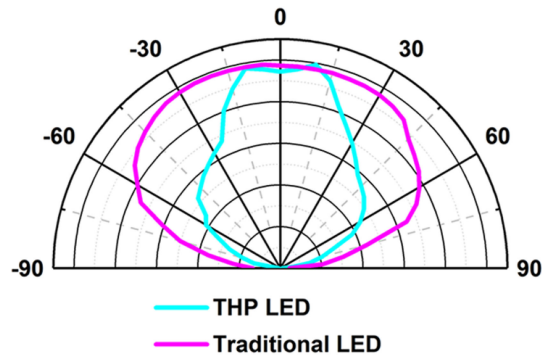
Fig. 3. The far-field beam profile of THP LED and traditional LED at a driving current of 350 mA.
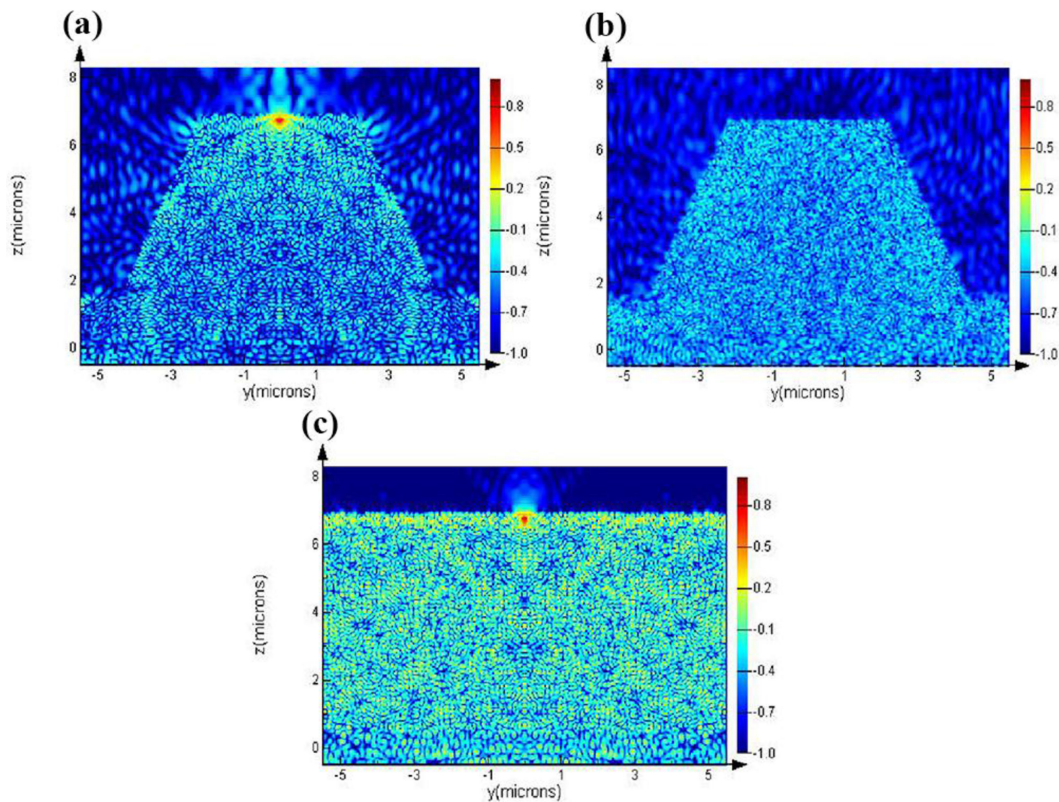

Fig. 4. The simulated emission patterns with the cross-section electrical field distributions when the light sources are on the side of (a) the c-plane as well as (b) the incline facets of the THP LED, and (c) the planar facet of the traditional LED, respectively.

Fig. 4(a)–(c) show the simulated cross-section electric field distribution when the light sources are set in the c-plane MQW as well as the incline facets MQW of the THP LED, and the planar facet MQW of the traditional LED, respectively. As shown in Fig. 4(c), for the traditional LED, photons emitting outside scope of the critical angle are completely reflected at the GaN/air planar interface. Thus, most of the light emitted from MQWs is trapped within the GaN layer, resulting in the huge light loss. On the contrary, for the THP LED, there are six inclined sidewalls and a c-plane. Each plane correspond to a different escaped cone. Therefore, compared with the traditional LED, the odds of light escaping from the THP LED is increased by six times. It can be observed from Fig. 4(a)
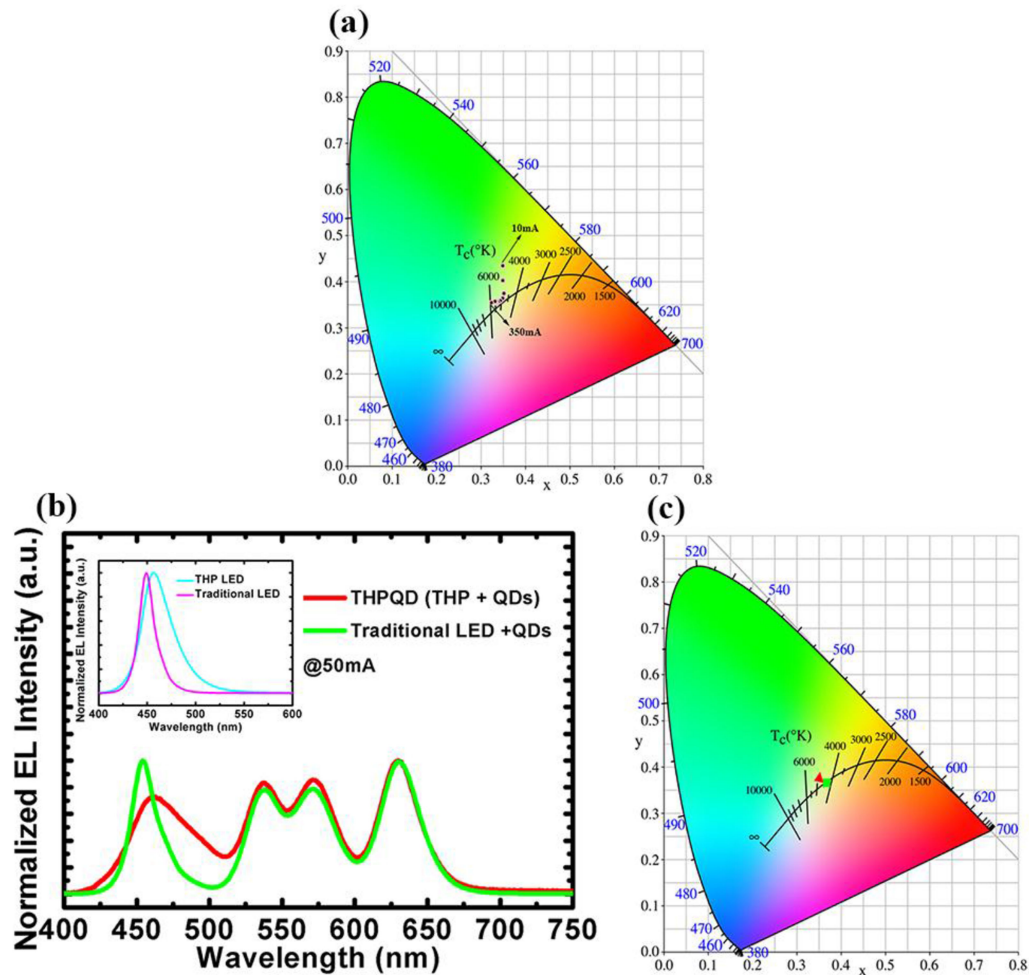
Fig. 5. (a) The variation coordinates in the CIE chromaticity diagram which are taken from the TH-PQD LED with the change of driving different current (10 ∼ 350 mA). (b) The relative spectrum of THPQD LED, the traditional LED with QDs under a current of 50 mA. (c) The coordinates of the THPQD LED as well as the traditional LED with QDs driven with 50 mA in the CIE chromaticity diagram, the THPQD LED is red triangle and the traditional LED with QDs is green square, respectively.

and 4(b) that the light is emitted from both the sidewall and c-plane. And the light also can be diffracted into the outside space by the interface between surfaces. As a result, the simulated light extraction efficiency are 78.51%, 72.76% for the c-plane MQW and the inclined facets MQW THP LED and 10.95% for the traditional LED, which reveals the light extraction efficiency of the THP LED is approximately 7 times as high as that of the traditional LED. The result indicates more light is extracted from the THP structures because total reflections are reduced by incorporating the THP structures.

However, the THP LED just realizes a broad wavelength range of light emission and still has a poor CRI because the spectrum does not completely cover the range of visible light. QDs have typical optical properties of narrow, tunable, symmetric emission spectrum and photochemically stable [30]–[32]. Therefore, we add a certain ratio of QDs into THP LED, so that the emission peaks can be broadened to increase the CRI. Fig. 5(a) shows the variation coordinates in the Commission Internationale de L'Éclairage (CIE) chromaticity diagram which are taken from THPQD LED after adding QDs under different currents (10 ∼ 350 mA). The range value of CRI is 71.2 ∼ 87.2. In addition, these points range from 4845 K to 5877 K in the correlated color temperature (CCT),

fully locating in the white region. The CRI firstly increases and then decreases with the increase of current. At a relatively low current, there is only one green peak. The blue peak appears when the current increases, and the spectrum becomes broadened, leading to the CRI increases. As the current continues to increase, the intensity of the blue and green peaks both increases. However, the blue peak is almost independent of the injection current, whereas the green peak is blue-shifted. Thus, it will lead to the fact that the spectrum becomes narrowed, resulting in the decrease of the CRI. It can be concluded that the broader the spectrum is, the higher is the value of the CRI.

The inset of Fig. 5(b) shows the normalized spectrum of the THP LED and the traditional LED under a current of 50 mA. It can be seen that the spectrum of THP LED is wider than that of the traditional LED. After adding QDs, the THPQD LED is wider than the traditional LED with QDs as shown in Fig. 5(b). Its spectrum cover the visible range, and is very close to the ideal white LED. The white emission of the THPQD LED has a high CRI value of $R_a = 87.2$ with $T_c = 4845$ K, which is located at (0.3518, 0.3741) in the 1931 CIE chromaticity diagram as shown in Fig. 4(c) (the red triangle). The CRI of the THPQD LED is high in comparison to the traditional white LED with QDs, which has CRI value of $R_a = 79.2$ (the green square). And the THPQD LED and the traditional LED with QDs are wider than that of the traditional phoshors-based white LED (traditional LED + yellow phoshors) which has CRI value of $R_a \approx 74$. It also indicates the THPQD LED could be used as a white LED to replace the incandescent lamp.

4. Conclusions

In summary, the phosphor-free three dimensional hybrid white LED device with the combination of the THP structures and QDs has been successfully fabricated. THP LED not only broadens the spectrum, but also makes the far-field viewing angle decrease by $\sim 45.4°$ and improves the light extraction efficiency compared with traditional LED. At the same time, we also use 3D-TDFD simulation to verify that the light extraction efficiency has been effectively improved. Furthermore, contrary to the traditional designs of 3D structures, the THPQD LED has a high CRI which cover more the range of visible light. The THPQD LED has been realized with a high CRI above 71.2, up to 87.2, covering different CCT ranging from 4845 K $\sim$ 5877 K, which closes to the ideal white LED. We expect this approach to be a promising candidate for producing highly efficient phosphor-free white LEDs with a high CRI.

References

[1] D. Min, D. Park, J. Jang, K. Lee, and O. Nam, "Phosphor-free white-light emitters using in-situ GaN nanostructures grown by metal organic chemical vapor deposition," *Sci. Rep.*, vol. 5, pp. 17372-1–17372-8, Dec. 2015.

[2] H. W. Lin, Y. J. Lu, H. Y. Chen, H. M. Lee, and S. Gwo, "InGaN/GaN nanorod array white light-emitting diode," *Appl. Phys. Lett.*, vol. 97, no. 7, pp. 073101-1–073101-3, Aug. 2010.

[3] M. Saha, A. Biswas, and H. Karan, "Monolithic high performance InGaN/GaN white LEDs with a tunnel junction cascaded yellow and blue light-emitting structures," *Opt. Mater.*, vol. 77, pp. 104–110, Jan. 2018.

[4] J. Ziegler *et al.*, "Silica-coated InP/ZnS nanocrystals as converter material in white LEDs," *Adv. Mater.*, vol. 20, pp. 4068–4073, 2008.

[5] F. Wang, Y. H. Chen, C. Y. Liu, and D. G. Ma, "White light-emitting devices based on carbon dots' electroluminescence," *Chem. Commun.*, vol. 47, pp. 3502–3504, Jan. 2011.

[6] Y. Zhuang *et al.*, "Effect of phosphor sedimentation on photochromic properties of a warm white light-emitting diode," *J. Semicond.*, vol. 39, no. 12, pp. 124006-1–124006-5, Dec. 2018.

[7] X. Guo, G. D. Shen, B. L. Guan, X. L. Gu, D. Wu, and Y. B. Li, "Cascade single-chip phosphor-free white light-emitting diodes," *Appl. Phys. Lett.*, vol. 92, no. 1, pp. 013507-1–013507-3, Jan. 2008.

[8] Z. Zhuang *et al.*, "High color rendering index hybrid III-nitride/nanocrystals white light-emitting diodes," *Adv. Funct. Mater.*, vol. 26, pp. 36–43, 2016.

[9] S. C. Shei, J. K. Sheu, C. M. Tsai, W. C. Lai, M. L. Lee, and C. H. Kuo, "Emission mechanism of mixed-color InGaN/GaN multi-quantum-well light-emitting diodes," *Jpn. J. Appl. Phys.*, vol. 45, no. 4A, pp. 2463–2466, Apr. 2006.

[10] I. K. Park, J. Y. Kim, M. K. Kwon, C. Y. Cho, J. H. Lim, and S. J. Park, "Phosphor-free white light-emitting diode with laterally distributed multiple quantum wells," *Appl. Phys. Lett.*, vol. 92, no. 9, pp. 091110-1–091110-3, Mar. 2008.

[11] K. Wu *et al.*, "Phosphor-free nanopyramid white light-emitting diodes grown on {101-1} planes using nanospherical-lens photolithography," *Appl. Phys. Lett.*, vol. 103, no. 24, pp. 241107-1–241107-5, Dec. 2013.

[12] M. L. Lee, Y. H. Yeh, S. J. Tu, P. C. Chen, W. C. Lai, and J. K. Sheu, "White emission from non-planar InGaN/GaN MQW LEDs grown on GaN template with truncated hexagonal pyramids," *Opt. Exp.*, vol. 23, no. 7, pp. A401–A412, Mar. 2015.

[13] K. Wu *et al.*, "Fabrication and optical characteristics of phosphor-free InGaN nanopyramid white light emitting diodes by nanospherical-lens photolithography," *J. Appl. Phys.*, vol. 115, no. 12, pp. 123101-1–123101-6, Mar. 2014.

[14] R. M. Farrell, E. C. Young, F. Wu, S. P. Denbaars, and J. S. Speck, "Materials and growth issues for high-performance nonpolar and semipolar light-emitting devices," *Semicond. Sci. Technol.*, vol. 27, pp. 024001-1–024001-14, Sep. 2012.

[15] G. F. Yang *et al.*, "InGaN/GaN multiple quantum wells on selectively grown GaN microfacets and the applications for phosphor-free white light-emitting diodes," *Rev. Phys.*, vol. 1, pp. 101–119, Jun. 2016.

[16] L. K. Aagesen, M. E. C. J. Han, and K. Thornton, "Phase-field simulations of GaN growth by selective area epitaxy from complex mask geometries," *J. Appl. Phys.*, vol. 117, no. 19, pp. 194302-1–194302-14, May 2015.

[17] Y. Zhao, H. Fu, G. T. Wang, and S. Nakamura, "Toward ultimate efficiency: Progress and prospects on planar and 3D nanostructured nonpolar and semipolar InGaN light-emitting diodes," *Adv. Opt. Photon.*, vol. 10, no. 1, pp. 246–308, Mar. 2018.

[18] S. Schwaiger *et al.*, "Planar semipolar (101-1) GaN on (112-3) sapphire," *Appl. Phys. Lett.*, vol. 96, no. 23, pp. 231905-1–231905-3, Jun. 2010.

[19] T. Fujii, Y. Gao, R. Sharma, E. L. Hu, S. P. DenBaars, and S. Nakamuraa, "Increase in the extraction efficiency of GaN-based light-emitting diodes via surface roughening," *Appl. Phys. Lett.*, vol. 84, no. 6, pp. 855–857, Dec. 2004.

[20] S. H. Lim, Y. H. Ko, C. Rodriguez, S. H. Gong, and Y. H. Cho, "Electrically driven, phosphor-free, white light-emitting diodes using gallium nitride-based double concentric truncated pyramid structures," *Light Sci. Appl.*, vol. 5, pp. e16030-1–e16030-6, Feb. 2016.

[21] Y. H. Ko, J. Song, B. Leung, J. Han, and Y. H. Cho, "Multi-color broadband visible light source via GaN hexagonal annular structure," *Sci. Rep.*, vol. 4, pp. 5514-1–5514-5, Jul. 2014.

[22] B. Fu *et al.*, "Phosphor-free InGaN micro-pyramid white light emitting diodes with multilayer graphene electrode," *RSC Adv.*, vol. 5, pp. 100646–100650, Nov. 2015.

[23] M. L. Lee *et al.*, "Dual-wavelength GaN-based LEDs grown on truncated hexagonal pyramids formed by selective-area regrowth on Si-implanted GaN templates," *Opt. Exp.*, vol. 21, no. S5, pp. A864–A871, Aug. 2013.

[24] G. Yang, P. Chen, S. Gao, G. Chen, R. Zhang, and Y. Zheng, "White-light emission from InGaN/GaN quantum well microrings grown by selective area epitaxy," *Photon. Res.*, vol. 4, no. 1, pp. 17–20, Jan. 2016.

[25] Y. C. Sim *et al.*, "Three-dimensional GaN dodecagonal ring structures for highly efficient phosphor-free warm white light-emitting diodes," *Nanoscale*, vol. 10, pp. 4686–4695, Jan. 2018.

[26] J. Kang *et al.*, "Pyramid array InGaN/GaN core-shell light emitting diodes with homogeneous multilayer graphene electrodes," *Appl. Phys. Exp.*, vol. 6, pp. 072102-1–072102-4, Jun. 2013.

[27] C. Y. Cho *et al.*, "InGaN/GaN multiple quantum wells grown on microfacets for white-light generation," *Appl. Phys. Lett.*, vol. 93, no. 24, pp. 241109-1–241109-3, Dec. 2008.

[28] D. Min, D. Park, K. Lee, and O. Nam, "Colour-crafted phosphor-free white light emitters via in-situ nanostructure engineering," *Sci. Rep.*, vol. 7, pp. 44148-1–44148-9, Mar. 2017.

[29] T. Wei *et al.*, "Selectively grown photonic crystal structures for high efficiency InGaN emitting diodes using nanospherical-lens lithography," *Appl. Phys. Lett.*, vol. 101, no. 21, pp. 211111-1–211111-5, Nov. 2012.

[30] W. K. Bae, K. Char, H. Hur, and S. Lee, "Single-step synthesis of quantum dots with chemical composition gradients," *Chem. Mater.*, vol. 20, no. 2, pp. 531–539, Jan. 2008.

[31] M. Bruchez, M. Moronne, P. Gin, S. Weiss, and A. P. Alivisatos, "Semiconductor nanocrystals as fluorescent biological labels," *Science*, vol. 281, no. 25, pp. 2013–2015, Oct. 1998.

[32] Y. Xie *et al.*, "Synthesis of highly stable quantum-dot silicone nanocomposites via in situ zinc-terminated polysiloxane passivation," *Nanoscale*, vol. 9, pp. 16836–16842, Oct. 2017.